# Seismic full waveform inversion in archaeological prospecting

**Daniel Köhn[1*], Manuel Zolchow[1], Rebekka Mecking[2], Dennis Wilken[1], Tina Wunderlich[1], Denise De Nil[1], Wolfgang Rabbel[1]**

1 Institute of Geosciences, Kiel University, Kiel, Germany
2 TEECsolutions, Isernhagen, Germany
* Corresponding author: E-mail: daniel.koehn@ifg.uni-kiel.de

**Abstract**
Seismic full waveform inversion is introduced as a novel high-resolution imaging tool in archaeological prospection. The full waveform inversion approach allows the high-resolution characterization of low-contrast sedimentary layers, high-contrast stone wall structures and air-filled cavities.

**Keywords**
archaeological prospection; full waveform inversion; seismic; subsurface characterization

## Introduction

Archaeological prospection can rely on a wide spectrum of electro/magnetic and seismic methods with different areal coverage. Elastic properties of the sub-surface are traditionally estimated by first arrival travel time tomography (FATT) or the inversion of surface wave dispersion spectra. Both of these approaches focus on special properties of the wavefield and therefore have limitations in terms of resolution and applicability. By incorporating phase and amplitude information of the entire recorded wavefield, the seismic full waveform inversion (FWI) is able to improve the structural resolution significantly. Previous studies demonstrated the capability of FWI to resolve near surface structures related to problems in engineering geophysics (Tran et al. 2013) and archaeogeophysics (Dokter et al. 2017; Wittkamp et al. 2018; Schwardt et al. 2020). In this presentation, we review some of our FWI applications in archaeogeophysics with different degrees of complexity and fields of application. Archaeological excavations allowed a ground truthing of the resulting subsurface models.

## Full waveform inversion approach

In seismic SH-FWI, the waveform misfit between modelled and field data is minimized in order to obtain high resolution models of the shear wave velocity vs and density distribution in the subsurface. To solve this non-linear optimization problem an appropriate objective function has to be defined. To mitigate common problems of applying 2D FWI to field data, like variable coupling at different receiver positions, we use the trace normalized global correlation norm GCN (Choi and Alkhalifah 2012; Dokter et al. 2017) to avoid these problems at least to some extent. This objective function can be minimized by iteratively updating the model parameters starting with an initial background model using a preconditioned conjugate gradient method (Dokter et al. 2017). To reduce the non-linearity of the inverse problem and mitigate the dominance of the low-frequency Love wave in favour of high-frequency data, a sequential FWI workflow of low-pass and band-pass filtered data with different bandwidth is applied (Köhn et al. 2019). Smoothness constraints are imposed by preconditioning the gradients with an anisotropic 2D Gaussian filter adapted to the local S-wavelength.

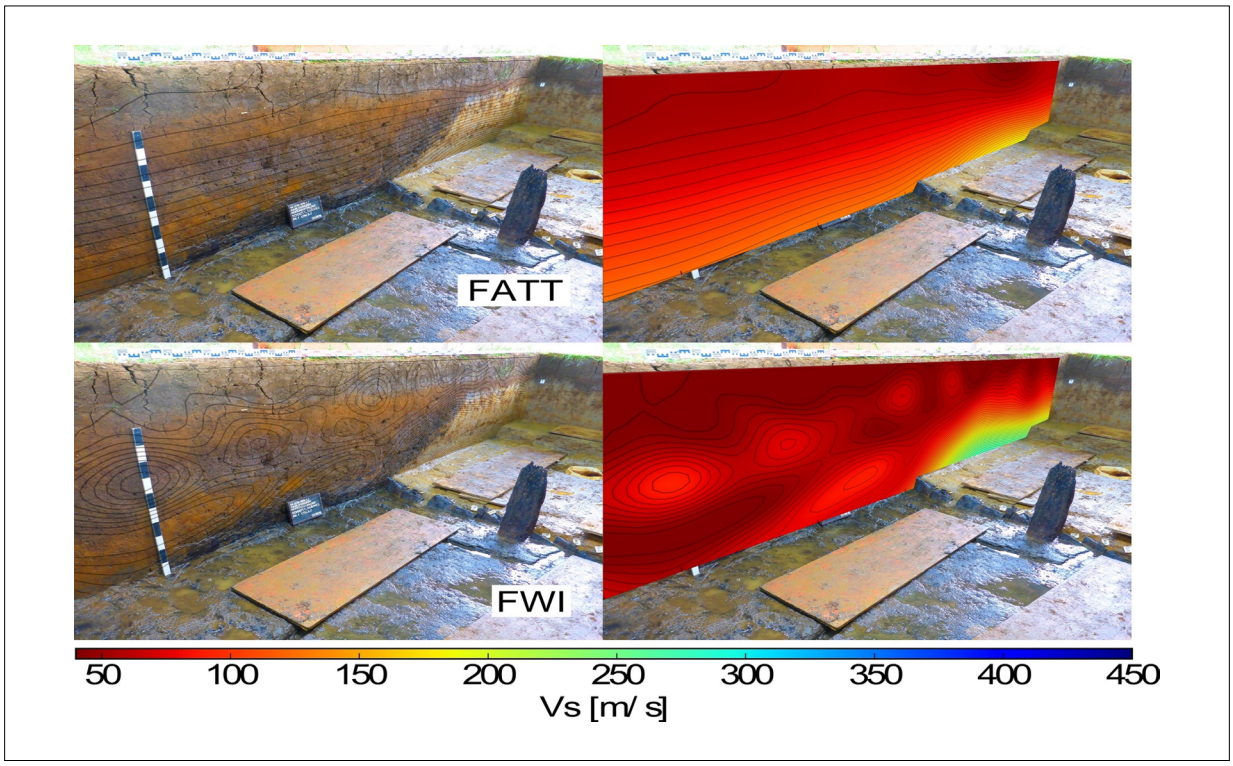


**Fig. 1:** Comparison of the Fossa Carolina canal structure from an excavation photo with FATT (top) and FWI results (bottom), respectively. The color bar is only related to the FATT/FWI results. Photo from Köhn et al. (2019).

## High resolution mapping of a near-surface canal structure

To demonstrate the potential of our SH-FWI approach, we inverted a SH-transect across the medieval Fossa Carolina canal structure (also known as "Karlsgraben") in southern Germany (Köhn et al. 2019). Originally initiated by the Franconian king Charlemagne as a 3 km long canal to connect the Danube and Rhine River system, the construction was realized in 793 AD. The Fossa Carolina is one of the most important major hydraulic engineering projects in the Early Middle Ages. An archaeological excavation (Schmidt et al. 2019) from August 2016 allowed a ground truthing of the FWI result. Figure 1 shows a comparison between an excavation photo and S-wave velocity models derived by First Arrival Travel-time Tomography (FATT) and FWI, respectively. The upper 40 cm of the depth-cut show a weathering layer consisting of soil and vertical cracks. With increasing depth alternating, distinct yellowish and grey clay layers are visible. Near the bottom of the excavation, parts of a black organic-rich layer define the shape of the canal basement. The FATT result (top) shows a gradual increase of the S-wave velocities with depth but no clear correlation with the true grey and yellowish subsurface layers. A slightly stronger velocity gradient appears at the sharp layer transition of the canal basement, but its shape is not accurately mapped by the FATT. The subsurface resolution is significantly improved by the FWI (bottom). The canal basement shape in the FWI result is defined by dense velocity contours, which indicate a significant velocity gradient. In contrast to the FATT, some distinct low- and high velocity anomalies appear within the canal. In some parts, colours of the photo can be directly correlated with the velocity model. For example, some low-velocity contour lines of the FWI Vs-model nearly coincide with a yellowish clay layer at the bottom left of the excavation, the high velocity anomaly above correlates with a grey clay layer. In the weathering layer this correlation is not so obvious anymore, because the loose soil and deep-penetrating vertical cracks lead to a reduction of the shear modulus. As a result, some dominant near surface low-velocity anomalies, down to a depth of 40 cm, are introduced.


KIEL-UP • DOI: https://doi.org/10.38072/978-3-928794-83-1/p4

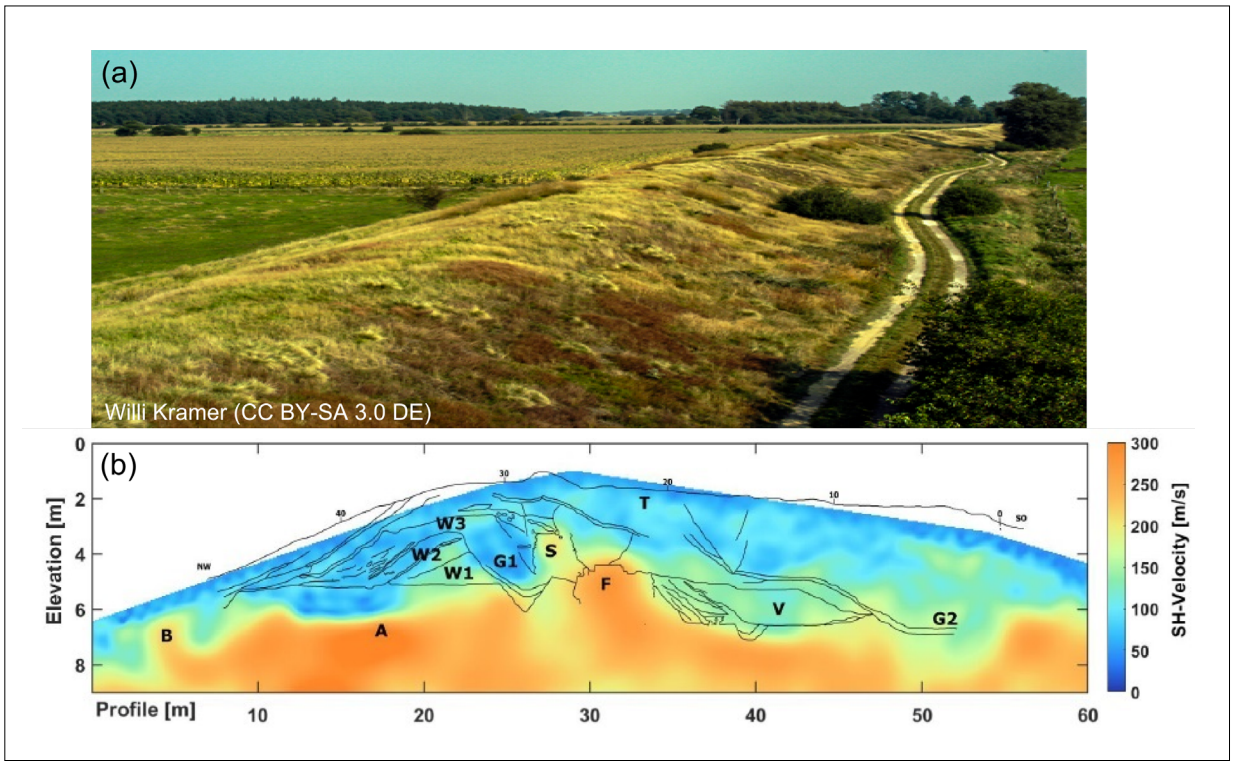


**Fig. 2:** Photo of the Danewerk (a) and ground truthing of the final FWI result in comparison with an archaeological excavation sketch (b) according to Andersen (1998). Prominent features: top layer (T), stone wall (S), wall foundations (F), early wall phases (W1-3), trench structures (G1-2), infilling (V),possible deeper foundations (A, B).

## FWI in the presence of significant surface topography

Significant surface topography poses a problem for FWI applications, due to the required accurate numerical modelling of synthetic surface wavefields, affected by the free-surface boundary condition. To solve this issue, a spatially oversampled Cartesian Finite-Difference approach with a special treatment of the free-surface boundary condition (Pan et al. 2018) is applied. An example of a problem with significant surface topography is the UNESCO World Heritage site Danewerk, a prominent defensive fortification wall, extending from the Baltic Sea to the North Sea in Northern Germany (Fig. 2 a). Originally built at some time before AD 500, the fortification was improved over the centuries by a wooden fence, a cobble stone wall and a massive brick stone wall. From a geophysical prospecting perspective, this target is especially interesting, because the embedded stone walls lead to significant physical parameter contrasts in the subsurface. Ground truthing of the FWI results is based on an excavation conducted in 1991 (Andersen 1998). Figure 2 b) shows a comparison between the FWI result and an archaeological sketch. Prominent features are marked by letters. W1, W2, W3, denote the different early, construction phases of the Danewerk. Initially, it was a small wall consisting only of soil growing over the centuries in size. W1 belongs to the oldest part of the Danewerk construction, while W2 and W3 were added later. The early construction phases W1, W2, W3 consist of soil with intermediate S-wave velocities between 150 m/s - 200 m/s. S denotes the remains of the cobble-stone wall which is also visible in the FWI results with S-wave velocities of 200 m/s. The compact brick-stone wall, denoted by F, can be characterized by higher velocities of about 300 m/s. Two high-velocity anomalies A and B with up to 400 m/s could be related to basement structures consisting of cobble stones to avoid a further collapse of the Danewerk.

## Detection of air-filled cavities

Another important field of application for the FWI is the detection of cavities. Figure 3a shows the Yigma Tepe, a monumental burial mound in the urban area of the an-

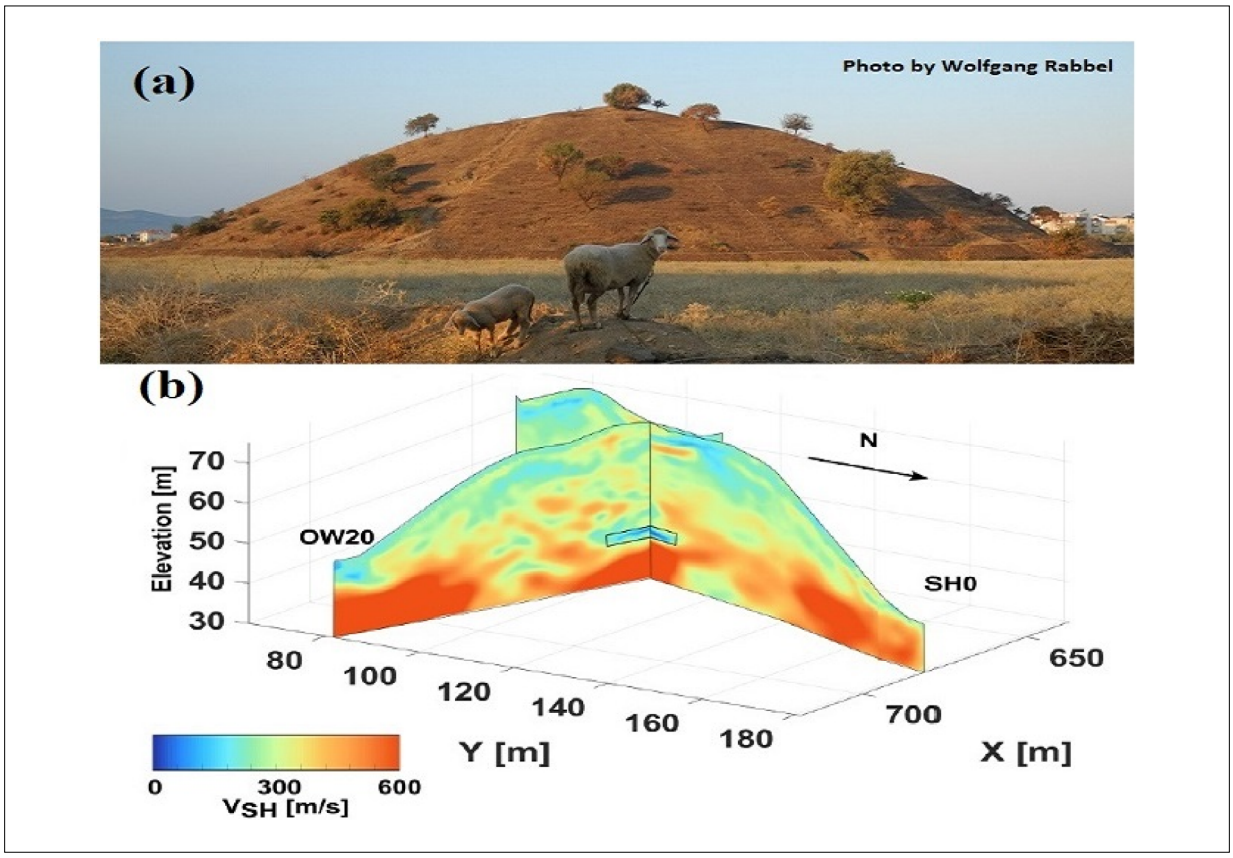


**Fig. 3:** Photo of the Yigma Tepe (a) and the 2D-FWI results of two SH-profiles along the mound (b).

cient city of Pergamon (Turkey). It is an almost circular structure with a diameter of 158 m and a height of about 32 m. The construction of the tumulus has been dated back to the Hellenistic period around 200 BC. The independent, reflection-focussed SH-FWI of two intersecting profiles across the tumulus (Mecking et al. 2021), revealed the complex internal structure of the mound and a prominent low-velocity anomaly at 30 m depth. This anomaly can be correlated with a system of partially collapsed excavation tunnels from the beginning of the 20th century. Notice also, that despite the 3D, heterogeneous subsurface structures, the 2D SH-FWI was able to resolve similar S-wave velocity anomalies at the intersection point of the two seismic profiles.

## Conclusions

In this talk, we demonstrated the potential of 2D SH-FWI to resolve near-surface structures, either low-contrast sedimentary layers, high-contrast stone wall structures or air-filled cavities in a 3D heterogeneous subsurface. The applicability of the developed 2D SH-FWI workflow is not limited to archaeological problems, but can also be adapted in the fields of engineering, geotechnical and non-destructive testing.

## Acknowledgments

The presented studies have been funded by the German Research Foundation (DFG), German Archaeological Institute (DAI), the German Federal Ministry of Education and Research (BMBF)/German Federal Ministry for Economic Affairs and Energy (BMWi). We thank all students, who participated in the archaeogeophysical survey campaigns and the developers/contributors to our Open Source 2D SH-FWI code DENISE, which is available under the terms of GNU GPL 2.0 at https://github.com/daniel-koehn.

## References

Andersen H. Danevirke og Kovirke. Arkæologiske undersøgelser 1861–1993. Aarhus University Press; 1998. Danish.

Choi Y, Alkhalifah T. Application of multi-source waveform inversion to marine streamer data using the global correlation norm. Geophysical Prospecting. 2012;60:748–758. doi: 10.1111/j.1365-2478.2012.01079.x

Dokter E, Köhn D, Wilken D, De Nil D, Rabbel W. Full-waveform inversion of SH- and Love-wave data in near-surface prospecting. Geophysical Prospecting. 2017;65(S1):216–236. doi: 10.1111/1365-2478.12549

Köhn D, Wilken D, De Nil D, Wunderlich T, Rabbel W, Werther L, et al. Comparison of time-domain SH waveform inversion strategies based on sequential low and bandpass filtered data for improved resolution in near-surface prospecting. Journal of Applied Geophysics. 2019;160:69–83. doi: 10.1016/j.jappgeo.2018.11.001

Mecking R, Köhn D, Meinecke M, Rabbel W. Cavity detection by SH-wave Full Waveform Inversion - A reflection-focused approach. Geophysics. 2021; 86(3):WA123-WA137. doi: 10.1190/geo2020-0349.1

Pan Y, Gao L, Bohlen T. Time-domain full-waveform inversion of Rayleigh and Love waves in presence of free-surface topography. Journal of Applied Geophysics. 2018;152:77–85. doi: 10.1016/j.jappgeo.2018.03.006

Schmidt J, Rabiger-Völlmer J, Werther L, Werban U, Dietrich P, Berg S, et al. 3D-Modelling of Charlemagne's Summit Canal (Southern Germany) -Merging Remote Sensing and Geoarchaeological Subsurface Data. Remote Sensing. 2019; 11(9): 1111. doi: 10.3390/rs11091111

Schwardt M, Köhn D, Wunderlich T, Wilken D, Seeliger M, Schmidts T, et al. Characterization of silty to fine-sandy sediments with SH waves: full waveform inversion in comparison with other geophysical methods. Near Surface Geophysics. 2020; 18(3): 217–248. doi: 10.1002/nsg.12097

Tran K, McVay M, Faraone M, Horhota D. Sinkhole detection using 2D full seismic waveform tomography. Geophysics. 2013; 78(5): R175–R183. doi: 10.1190/geo2013-0063.1

Wittkamp F, Athanasopoulos N, Bohlen T. Individual and joint 2-D elastic full-waveform inversion of Rayleigh and Love waves. Geophysical Journal International. 2018;216(1):350–364. doi: 10.1093/gji/ggy432